Journal of Nuclear Medicine, published on July 17, 2020 as doi:10.2967/jnumed.120.247882

Head-to-head evaluation of ^{18}F-FES and ^{18}F-FDG PET/CT in metastatic invasive lobular breast cancer

Gary A. Ulaner[1,2], Komal Jhaveri[3,4], Sarat Chandarlapaty[3,4], Vaios Hatzoglou[1,2], Christopher C. Riedl[1,2], Jason S. Lewis[1,2], and Audrey Mauguen[5]

Departments of [1]Radiology, [3]Medicine, and [5]Epidemiology & Biostatistics, Memorial Sloan Kettering Cancer Center, New York, NY
Departments of [2]Radiology and [4]Medicine, Weill Cornell Medical College, New York, NY

Financial support: Susan G. Komen for the Cure Research Grant KG110441 (GAU). This research was funded in part through the NIH/NCI Cancer Center Support Grant P30 CA008748. No potential conflicts of interest relevant to this article exist.

Corresponding author and first author:
Gary A. Ulaner, MD, PhD
Department of Radiology, MSK
Tel: +1-212-639-3776
Fax: 212-717-3263
E-mail: ulanerg@mskcc.org

Running title: FES vs. FDG in ILC

ABSTRACT

Invasive lobular carcinoma (ILC) demonstrates lower conspicuity on 2-deoxy-2-^{18}F-fluoro-D-glucose (^{18}F-FDG) PET than the more common invasive ductal carcinoma (IDC). Other molecular imaging methods may be needed for evaluation of this malignancy. As ILC is nearly always (95%) estrogen receptor (ER) positive, ER-targeting PET tracers such as 16α-^{18}F-fluoroestradiol (18F-FES) may have value. We reviewed prospective trials at Memorial Sloan Kettering Cancer Center (MSK) utilizing 18F-FES PET/CT to evaluate metastatic ILC patients with synchronous ^{18}F-FDG and ^{18}F-FES PET/CT imaging, which allowed a head-to-head comparison of these two PET tracers.

Methods: Six prospective clinical trials utilizing ^{18}F-FES PET/CT in patients with metastatic breast cancer were performed at MSK from 2008-2019. These trials included 92 patients, of which 14 (15%) were of ILC histology. Seven of 14 patients with ILC had an ^{18}F-FDG PET/CT performed within 5 weeks of the research ^{18}F-FES PET/CT and no intervening change in management. For these 7 patients, the ^{18}F-FES and ^{18}F-FDG PET/CT studies were analyzed to determine the total number of tracer avid lesions, organ systems of involvement, and SUVmax of each organ system for both tracers.

Results: In the seven comparable pairs of scans, there were a total of 254 ^{18}F-FES-avid lesions (SUVmax 2.6 to 17.9) and 111 ^{18}F-FDG-avid lesions (SUVmax 3.3 to 9.9) suspicious for malignancy. For 5 of 7 (71%) of ILC patients, ^{18}F-FES PET/CT detected more metastatic lesions than ^{18}F-FDG PET/CT. In the same 5 of 7 patients, the SUVmax of ^{18}F-FES-avid lesions was greater than the SUVmax of ^{18}F-FDG-avid lesions. One patient had ^{18}F-FES avid metastases with no corresponding ^{18}F-FDG avid metastases. There were no patients with ^{18}F-FDG avid distant metastases without ^{18}F-FES avid distant metastases, although in one patient liver metastases were evident on ^{18}F-FDG but not ^{18}F-FES PET.

Conclusion: ^{18}F-FES PET/CT compared favorably with ^{18}F-FDG PET/CT for detection of metastases in patients with metastatic ILC. Larger prospective trials of ^{18}F-FES PET/CT in ILC should be considered to evaluate ER-targeted imaging for clinical value in patients with this histology of breast cancer.

Keywords: Lobular, breast cancer, ^{18}F-FES, ^{18}F-FDG, PET/CT

INTRODUCTION

2-deoxy-2-^{18}F-fluoro-D-glucose (^{18}F-FDG) PET/CT plays an important role in the management of patients with breast cancer (*1,2*). The impact of ^{18}F-FDG PET/CT in patients with breast cancer differs between the most common histology of breast cancer, invasive ductal carcinoma (IDC, 80% of breast cancers) and the second most common histology, invasive lobular carcinoma (ILC, 10-15% of breast cancers) (*3,4*). Due to distinct molecular and pathologic features (*5,6*), including lower cellular density per unit volume, ILC is more difficult to detect on imaging, including mammography, ultrasound, magnetic resonance imaging, and ^{18}F-FDG PET/CT (*7-16*). Both primary and metastatic ILC demonstrates lower standard uptake values (SUVs) on ^{18}F-FDG PET than comparable IDC tumors (*11-16*). In addition, ILC differs in its patterns of metastatic spread when compared with IDC (*17-20*). Given these differences, ^{18}F-FDG PET/CT may be less suited for evaluation of ILC than IDC (*16*).

ILC also differs from IDC in receptor expression. In particular, ILC is nearly always (95%) estrogen receptor (ER)-positive (*5,21,22*). This raises the possibility of increased utility of ER-targeting PET tracers for patients with ILC. ^{18}F-fluoroestradiol (^{18}F-FES) is an ER-targeting PET tracer with high sensitivity and specificity for detection of ER-positive tumors (*23-27*). ^{18}F-FES has been utilized as a predictive biomarker (*28-31*) to demonstrate ER heterogeneity (*32,33*), assess pharmacokinetics of ER-targeted agents (*34*), measure residual ER during endocrine therapy (*35*), and determine biologic optimal dose of novel ER-targeted drugs (*36*).

We hypothesized that due to high ER positivity, ^{18}F-FES PET/CT may compare favorably to ^{18}F-FDG PET/CT in patients with ILC. Prospective trials have been conducted at Memorial Sloan Kettering using ^{18}F-FES PET/CT to assist in determining dose of novel ER-

targeted drugs. We reviewed these trials for patients with ILC who underwent ^{18}F-FDG PET/CT within five weeks of the research ^{18}F-FES PET/CT and had no intervening change in management. Here we report this head-to-head comparison of ^{18}F-FES and ^{18}F-FDG PET/CT in patients with metastatic ILC.

MATERIALS AND METHODS

Patients

This retrospective evaluation of prospective clinical trials was performed in compliance with the Health Insurance Portability and Accountability Act and with Institutional Review Board approval. All patients provided written informed consent. Six prospective clinical trials utilizing ^{18}F-FES PET/CT in patients with breast cancer (NCT trial numbers: 01823835, 01916122, 02316509, 02734615, 03284957, and 03332797) were reviewed for patients with metastatic invasive lobular breast cancer and standard-of-care ^{18}F-FDG PET/CT performed within five weeks of research ^{18}F-FES PET/CT and who had no change in therapeutic management between scans. Both the research FES-PET/CT and standard-of-care FDG-PET/CT studies were performed prior to therapy without intervening change in patient management.

Electronic medical records were reviewed for age at ^{18}F-FES PET/CT, gender, and receptor status (estrogen receptor (ER), progesterone receptor (PR), and human growth factor receptor 2 (HER2)), as well as number of days between the ^{18}F-FES and ^{18}F-FDG PET/CT scans.

PET/CT Imaging and Interpretation

All patients in this study had synchronous ^{18}F-FDG PET/CT and ^{18}F-FES PET/CT as defined above. Studies were reinterpreted by a radiologist (G.U.) dually boarded in diagnostic radiology and nuclear medicine with 15 years of PET/CT experience, including experience in both agents.

^{18}F-FES PET/CT performance was standardized in all studies according to a registered clinical trial (NCT01916122). ^{18}F-FES was manufactured by the Radiochemistry and Imaging Probe Core at MSK using a modified version of the published work by Knott et al, 2011 (*37*). Each patient was administered approximately 185 Mbq (5 mCi) of ^{18}F-FES intravenously, followed by a 60-minute uptake period. PET/CT scans were acquired supine from the base of the skull to the mid-thigh along with low-dose CT scans. Attenuation-corrected images were reviewed on a picture-archiving and communication system workstation (GE Healthcare, Chicago, Illinois). Physiologic ^{18}F-FES avidity was expected in the liver, bowel, kidney, and bladder. ^{18}F-FES avidity was considered abnormal when it was focal and not considered physiologic.

For ^{18}F-FDG PET/CT examinations, ^{18}F-FDG was obtained from a commercial source. Patients fasted for at least six hours prior to ^{18}F-FDG administration. Each patient was injected intravenously with 444-555 MBq (12-15 mCi) of ^{18}F-FDG when plasma glucose was less than 200 mg/dL, followed by a 60-minute uptake period. PET/CT scans were acquired supine from the base of the skull to the mid-thigh along with low-dose CT scans. Attenuation-corrected images were reviewed on a picture-archiving and communication system workstation. ^{18}F-FDG

avidity was considered abnormal when it was focal and not considered physiologic or inflammatory.

For both examinations, the organ systems with disease involvement, the number of disease foci in each organ system, and the SUVmax for lesions were recorded. SUVmax was determined by placement of regions of interest around the lesions with the greatest avidity. As lesions had different ^{18}F-FES and ^{18}F-FDG avidity, different lesions may be selected as the most avid for each study. Liver background SUVmax and mean values were determined by placement of regions of interest over a one-cubic-centimeter volume of the right lobe of the liver.

Statistics

Results were described using median and range. To assess whether the distribution of the number of lesions or the SUVmax was higher with ^{18}F-FES PET than ^{18}F-FDG PET, one-sided Wilcoxon signed rank tests for paired data were used. To account for the small sample size, results with a p-value <0.10 were considered statistically significant.

RESULTS

Patients

92 patients with breast cancer underwent ^{18}F-FES PET/CT as part of six prospective clinical trials. Seventy-eight (85%) were excluded for non-ILC histology. Seven (8%) were excluded for no comparison ^{18}F-FDG PET/CT. This resulted in seven evaluable patients. A Standards for Reporting of Diagnostic Accuracy Studies (STARD) diagram for patient selection is presented in Figure 1. The seven patients were all women with ER-positive, PR-positive, and HER2-negative ILC. The median age was 66 years (range 48-69 years). For all patients, the ^{18}F-FDG PET/CT was performed before the ^{18}F-FES PET/CT. The median time between scans was 19 days (range 11-35 days).

^{18}F-FES PET/CT

All seven patients demonstrated ^{18}F-FES-avid lesions consistent with metastases (Table 1). All demonstrated osseous metastases and one demonstrated a biopsy-proven breast recurrence. A total of 253 ^{18}F-FES-avid osseous lesions were seen. The range of ^{18}F-FES SUVmax values for osseous lesions among the seven patients was 2.6 to 17.9 (median = 10.2). There was one focus representing the breast recurrence in patient #3 with a ^{18}F-FES SUVmax of 6.5. Patient #5 demonstrated a focus in the right lung hilum (SUVmax 3.6), without correlate on CT, of unclear etiology. This was not included in the lesions suspicious for malignancy as the right hilum is unlikely to be a site of nodal metastases in a breast cancer patient without axillary

or internal mammary nodal metastases. No other organ systems were found to have suspicious ^{18}F-FES-avid foci.

^{18}F-FDG PET/CT

Six of seven patients demonstrated ^{18}F-FDG-avid lesions consistent with metastases (Table 1). Six demonstrated ^{18}F-FDG-avid osseous metastases, one demonstrated an ^{18}F-FDG-avid, biopsy-proven breast recurrence, and one demonstrated ^{18}F-FDG-avid hepatic metastases. A total of 90 ^{18}F-FDG-avid osseous lesions were seen. The range of ^{18}F-FDG SUVmax values of osseous lesions was 3.5 to 9.9 (median = 5.3). There was one focus representing the breast recurrence in patient #3 (the same lesion detected on ^{18}F-FES PET/CT) with an SUVmax of 3.3. Patient #7 demonstrated 20 ^{18}F-FDG-avid hepatic metastases with an SUVmax of 5.9. Patient #1 demonstrated ^{18}F-FDG avidity adjacent to a breast implant that was probably benign. No other organ systems were found to have suspicious ^{18}F-FDG-avid foci.

Comparison of ^{18}F-FES and ^{18}F-FDG PET/CT

In 5 of 7 patients (71%), ^{18}F-FES PET/CT detected more metastatic lesions than ^{18}F-FDG PET/CT (Table 1, Fig. 2). In these five patients, the SUVmax of ^{18}F-FES-avid lesions was greater than the SUVmax of ^{18}F-FDG-avid lesions.

A total of 268 osseous lesions were detected by either ^{18}F-FES or ^{18}F-FDG PET. Of 268 lesions, 253 (94%) were ^{18}F-FES-avid, while 90 of 268 (34%) were ^{18}F-FDG-avid. ^{18}F-FES PET

detected more osseous lesions (median = 14, range 2-146 lesions) than ^{18}F-FDG (median = 6, range 0-56, p = 0.08). In 6 of 7 patients, more osseous foci were detected on ^{18}F-FES PET than on ^{18}F-FDG PET. In one patient, two avid osseous metastases were seen on ^{18}F-FES PET, but no avid osseous metastases were detected on ^{18}F-FDG PET (patient #5, Table 1 and Fig. 2). This patient had extensive sclerotic osseous lesions on CT (Fig. 3) and known active osseous metastases from a biopsy used to enroll the patient on the prospective clinical trial. Patients could demonstrate heterogeneity of tracer avidity, with some osseous metastases that were avid for both tracers, while others were ^{18}F-FES-avid but not ^{18}F-FDG-avid, or vice versa (patient #7, Fig. 2). This resulted in the total number of osseous metastases detected in the study being higher than the total with either tracer alone.

Additionally, one patient (patient #7) demonstrated 20 ^{18}F-FDG-avid hepatic metastases that were not apparent on ^{18}F-FES PET (Table 1, Fig. 2). The detection of hepatic metastases is known to be more difficult of ^{18}F-FES PET due to the physiologic excretion of ^{18}F-FES by the liver. As expected, in the patients in our study, physiologic liver background was higher on ^{18}F-FES PET than on ^{18}F-FDG PET. The median (range) of physiologic liver background ^{18}F-FES SUVmax and SUVmean were 15.4 (12.5-22.9) and 13.8 (10.6-20.3), while the median (range) of physiologic liver background ^{18}F-FDG SUVmax and SUVmean were 2.8 (2.2-3.8) and 2.6 (1.9-3.5).

Figure 4 provides a visual depiction of the number of lesions detected on ^{18}F-FES PET/CT and ^{18}F-FDG PET/CT in each patient and a comparison of the lesional SUVmax for both radiotracers in each patient. Figure 5 provides a graphical demonstration of the SUVmax values for all lesions in all patients.

DISCUSSION

ILC is a histologic subtype of breast cancer with distinct molecular and imaging characteristics. Novel methods may be needed for optimal visualization of ILC. This study took advantage of prospective trials utilizing ^{18}F-FES to perform a head-to-head comparison between ^{18}F-FES and ^{18}F-FDG PET/CT in patients with metastatic ILC and demonstrated that ^{18}F-FES may compare favorably to ^{18}F-FDG in these patients.

ILC is sometimes thought of as a "rare" tumor type, but this is a misconception. While only 15% of all breast malignancies are ILC (*3,38*), 15% of 279,000 breast malignancies a year (*39*) represents 42,000 malignancies. If ILC was its own category of malignancy, it would be the fifth most common malignancy of women, behind only ductal breast cancer, lung, colon/rectum, and uterine cancer (*39*). Thus, ILC is common and improved imaging of this malignancy could have a major impact on health care.

^{18}F-FES PET is gaining increased recognition as a PET tracer with clinical applicability and has recently been approved by the United States Food and Drug Administration for evaluation of ER heterogeneity as EstroTep (Zionexa, Paris, France). This early study suggests that evaluation of metastatic ILC may be one clinical scenario where ^{18}F-FES PET/CT has clinical utility.

Molecular imaging has demonstrated advantages over anatomic imaging for osseous malignancies. As the attenuation/density of an osseous lesion must change 30-50% prior to being detected on CT (*40*), molecular techniques such as bone scan and ^{18}F-FDG PET are often more sensitive for detection of osseous malignancy (*41,42*). Due to limitations for anatomic imaging of osseous lesions, Response Criteria in Solid Tumors (RECIST) does not consider osseous lesions without soft tissue components to be eligible as target lesions (*43*). As the most common

site of distant metastasis in ILC is bone (*44*), it is important to have an imaging method that is sensitive for the detection of osseous disease. In this study, ^{18}F-FES PET was more sensitive than ^{18}F-FDG PET for osseous lesions on both a per-lesion and per-patient basis (Table 1). The detection of ^{18}F-FES-avid osseous lesions in ILC can assist with evaluation of extent of disease, and could be considered as a method to identify measurable lesions for clinical trials, similar to the recent use of ^{18}F-FDG PET imaging to expand trial eligibility in solid tumors with a predominance of osseous disease (*45*).

It is recognized that the liver is a site of weakness for ^{18}F-FES PET imaging due to the physiologic excretion of ^{18}F-FES through the hepatobiliary system. Thus, if ^{18}F-FES PET is utilized for patient care, the liver will need to be evaluated by an additional method, such as contrast-enhanced CT or MR.

Our study has several limitations. First and foremost was the limited number of patients. This is only an initial comparison of ^{18}F-FES and ^{18}F-FDG PET/CT in patients with metastatic ILC. As ^{18}F-FES PET/CT is not yet widespread, in addition to ILC only recently being recognized as a distinct breast cancer subtype requiring alternate methods of molecular imaging (*46-48*), limited the number of patients available for analysis. Second, in the patients in this manuscript, ^{18}F-FDG PET was always performed before ^{18}F-FES PET. Thus, there could have been some progression of disease in the 11-35 days between scans. Third, ^{18}F-FDG PET and ^{18}F-FES scans may not have been performed on the same PET/CT scanner. Fourth, this was a single-institution study. Finally, we do not have histological confirmation of imaging findings. While all patients were biopsy-proven to have metastatic ILC, we cannot guarantee each avid focus is a site of malignancy. However, ^{18}F-FES and ^{18}F-FDG PET/CT imaging findings were typical of findings for metastatic disease.

CONCLUSION

This retrospective review of prospective clinical trials utilizing ^{18}F-FES PET/CT provides the first head-to-head comparison of ^{18}F-FES PET/CT and ^{18}F-FDG PET/CT in patients with metastatic ILC. ^{18}F-FES PET compares favorably with ^{18}F-FDG for identifying sites of metastatic disease, particularly osseous metastases. As ILC is a malignancy in need of improved molecular imaging, larger trials should be considered to evaluate the clinical value of ^{18}F-FES PET/CT in these patients.

ACKNOWLEDGMENTS

This work was supported by a Susan Komen Grant KG110441 (GAU) and a NIH/NCI Cancer Center Support Grant P30 CA008748.

KEY POINTS

QUESTION: Does ^{18}F-FES PET/CT have value for evaluating disease in patients with lobular breast cancer?

PERTINENT FINDINGS: In this retrospective review of prospective clinical trials, FES demonstrated both more metastatic lesions and higher SUV values for malignancy than FDG in 71% of patients.

IMPLICATIONS: Our results support that a larger prospective trial of FES PET/CT in ILC is warranted to evaluate potential added clinical value in patients with ILC.

REFERENCES

1. NCCN Clinical Practice Guidelines in Oncology. Breast Cancer. Version 3.2019. www.nccn.org Published 2019.

2. Hildebrandt MG, Gerke O, Baun C, et al. [18F]Fluorodeoxyglucose (FDG)-Positron Emission Tomography (PET)/Computed Tomography (CT) in Suspected Recurrent Breast Cancer: A Prospective Comparative Study of Dual-Time-Point FDG-PET/CT, Contrast-Enhanced CT, and Bone Scintigraphy. *J Clin Oncol.* 2016;34:1889-1897.

3. Li CI, Anderson BO, Daling JR, Moe RE. Trends in incidence rates of invasive lobular and ductal breast carcinoma. *JAMA.* 2003;289:1421-1424.

4. Li CI, Uribe DJ, Daling JR. Clinical characteristics of different histologic types of breast cancer. *Br J Cancer.* 2005;93:1046-1052.

5. Ciriello G, Gatza ML, Beck AH, et al. Comprehensive Molecular Portraits of Invasive Lobular Breast Cancer. *Cell.* 2015;163:506-519.

6. Pestalozzi BC, Zahrieh D, Mallon E, et al. Distinct clinical and prognostic features of infiltrating lobular carcinoma of the breast: combined results of 15 International Breast Cancer Study Group clinical trials. *J Clin Oncol.* 2008;26:3006-3014.

7. Yoder BJ, Wilkinson EJ, Massoll NA. Molecular and morphologic distinctions between infiltrating ductal and lobular carcinoma of the breast. *Breast J.* 2007;13:172-179.

8. Bertucci F, Orsetti B, Negre V, et al. Lobular and ductal carcinomas of the breast have distinct genomic and expression profiles. *Oncogene.* 2008;27:5359-5372.

9. Berg WA, Gutierrez L, NessAiver MS, et al. Diagnostic accuracy of mammography, clinical examination, US, and MR imaging in preoperative assessment of breast cancer. *Radiology.* 2004;233:830-849.

10. Lopez JK, Bassett LW. Invasive lobular carcinoma of the breast: spectrum of mammographic, US, and MR imaging findings. *Radiographics.* 2009;29:165-176.

11. Avril N, Rose CA, Schelling M, et al. Breast imaging with positron emission tomography and fluorine-18 fluorodeoxyglucose: use and limitations. *J Clin Oncol.* 2000;18:3495-3502.

12. Avril N, Menzel M, Dose J, et al. Glucose metabolism of breast cancer assessed by 18F-FDG PET: histologic and immunohistochemical tissue analysis. *J Nucl Med.* 2001;42:9-16.

13. Bos R, van Der Hoeven JJ, van Der Wall E, et al. Biologic correlates of (18)fluorodeoxyglucose uptake in human breast cancer measured by positron emission tomography. *J Clin Oncol.* 2002;20:379-387.

14. Buck A, Schirrmeister H, Kuhn T, et al. FDG uptake in breast cancer: correlation with biological and clinical prognostic parameters. *Eur J Nucl Med Mol Imaging.* 2002;29:1317-1323.

15. Dashevsky BZ, Goldman DA, Parsons M, et al. Appearance of untreated bone metastases from breast cancer on FDG PET/CT: importance of histologic subtype. *Eur J Nucl Med Mol Imaging.* 2015;42:1666-1673.

16. Hogan MP, Goldman DA, Dashevsky B, et al. Comparison of 18F-FDG PET/CT for Systemic Staging of Newly Diagnosed Invasive Lobular Carcinoma Versus Invasive Ductal Carcinoma. *J Nucl Med.* 2015;56:1674-1680.

17. Lamovec J, Bracko M. Metastatic pattern of infiltrating lobular carcinoma of the breast: an autopsy study. *J Surg Oncol.* 1991;48:28-33.

18. Borst MJ, Ingold JA. Metastatic patterns of invasive lobular versus invasive ductal carcinoma of the breast. *Surgery.* 1993;114:637-641; discussion 641-632.

19. He H, Gonzalez A, Robinson E, Yang WT. Distant metastatic disease manifestations in infiltrating lobular carcinoma of the breast. *AJR Am J Roentgenol.* 2014;202:1140-1148.

20. Kane AJ, Wang ZJ, Qayyum A, Yeh BM, Webb EM, Coakley FV. Frequency and etiology of unexplained bilateral hydronephrosis in patients with breast cancer: results of a longitudinal CT study. *Clin Imaging.* 2012;36:263-266.

21. Chen Z, Yang J, Li S, et al. Invasive lobular carcinoma of the breast: A special histological type compared with invasive ductal carcinoma. *PLoS One.* 2017;12:e0182397.

22. McCart Reed AE, Kutasovic JR, Lakhani SR, Simpson PT. Invasive lobular carcinoma of the breast: morphology, biomarkers and 'omics. *Breast Cancer Res.* 2015;17:12.

23. Kurland BF, Peterson LM, Lee JH, et al. Estrogen Receptor Binding (18F-FES PET) and Glycolytic Activity (18F-FDG PET) Predict Progression-Free Survival on Endocrine Therapy in Patients with ER+ Breast Cancer. *Clin Cancer Res.* 2017;23:407-415.

24. van Kruchten M, de Vries EGE, Brown M, et al. PET imaging of oestrogen receptors in patients with breast cancer. *Lancet Oncol.* 2013;14:e465-e475.

25. Kurland BF, Peterson LM, Lee JH, et al. Between-patient and within-patient (site-to-site) variability in estrogen receptor binding, measured in vivo by 18F-fluoroestradiol PET. *J Nucl Med.* 2011;52:1541-1549.

26. Sundararajan L, Linden HM, Link JM, Krohn KA, Mankoff DA. 18F-Fluoroestradiol. *Semin Nucl Med.* 2007;37:470-476.

27. Linden HM, Peterson LM, Fowler AM. Clinical Potential of Estrogen and Progesterone Receptor Imaging. *PET Clin.* 2018;13:415-422.

28. Dehdashti F, Mortimer JE, Trinkaus K, et al. PET-based estradiol challenge as a predictive biomarker of response to endocrine therapy in women with estrogen-receptor-positive breast cancer. *Breast Cancer Res Treat.* 2009;113:509-517.

29. Peterson LM, Kurland BF, Schubert EK, et al. A phase 2 study of 16alpha-[18F]-fluoro-17beta-estradiol positron emission tomography (FES-PET) as a marker of hormone sensitivity in metastatic breast cancer (MBC). *Mol Imaging Biol.* 2014;16:431-440.

30. van Kruchten M, Glaudemans A, de Vries EFJ, Schroder CP, de Vries EGE, Hospers GAP. Positron emission tomography of tumour [(18)F]fluoroestradiol uptake in patients with acquired hormone-resistant metastatic breast cancer prior to oestradiol therapy. *Eur J Nucl Med Mol Imaging.* 2015;42:1674-1681.

31. Ulaner GA, Riedl CC, Dickler MN, Jhaveri K, Pandit-Taskar N, Weber W. Molecular Imaging of Biomarkers in Breast Cancer. *J Nucl Med.* 2016;57 Suppl 1:53S-59S.

32. Currin E, Peterson LM, Schubert EK, et al. Temporal Heterogeneity of Estrogen Receptor Expression in Bone-Dominant Breast Cancer: 18F-Fluoroestradiol PET Imaging Shows Return of ER Expression. *J Natl Compr Canc Netw.* 2016;14:144-147.

33. Nienhuis HH, van Kruchten M, Elias SG, et al. (18)F-Fluoroestradiol Tumor Uptake Is Heterogeneous and Influenced by Site of Metastasis in Breast Cancer Patients. *J Nucl Med.* 2018;59:1212-1218.

34. Linden HM, Kurland BF, Peterson LM, et al. Fluoroestradiol positron emission tomography reveals differences in pharmacodynamics of aromatase inhibitors, tamoxifen, and fulvestrant in patients with metastatic breast cancer. *Clin Cancer Res.* 2011;17:4799-4805.

35. van Kruchten M, de Vries EG, Glaudemans AW, et al. Measuring residual estrogen receptor availability during fulvestrant therapy in patients with metastatic breast cancer. *Cancer Discov.* 2015;5:72-81.

36. Wang Y, Ayres KL, Goldman DA, et al. 18F-Fluoroestradiol PET/CT Measurement of Estrogen Receptor Suppression during a Phase I Trial of the Novel Estrogen Receptor-Targeted Therapeutic GDC-0810: Using an Imaging Biomarker to Guide Drug Dosage in Subsequent Trials. *Clin Cancer Res.* 2017;23:3053-3060.

37. Knott K, Gratz D, Hubner S, Juttler S, Zankl C, Muller M. Simplified and automatic one-pot synthesis of 16α-[18F]fluoroestradiol without high-performance liquid chromatography purification. *Journal of Labelled Compounds and Radiopharmaceuticals.* 2011;54:749-753.

38. Eheman CR, Shaw KM, Ryerson AB, Miller JW, Ajani UA, White MC. The changing incidence of in situ and invasive ductal and lobular breast carcinomas: United States, 1999-2004. *Cancer Epidemiol Biomarkers Prev.* 2009;18:1763-1769.

39. Siegel RL, Miller KD, Jemal A. Cancer statistics, 2020. *CA Cancer J Clin.* 2020;70:7-30.

40. Vinholes J, Coleman R, Eastell R. Effects of bone metastases on bone metabolism: implications for diagnosis, imaging and assessment of response to cancer treatment. *Cancer Treat Rev.* 1996;22:289-331.

41. Iagaru A, Minamimoto R. Nuclear Medicine Imaging Techniques for Detection of Skeletal Metastases in Breast Cancer. *PET Clin.* 2018;13:383-393.

42. Peterson LM, O'Sullivan J, Wu QV, et al. Prospective Study of Serial (18)F-FDG PET and (18)F-Fluoride PET to Predict Time to Skeletal-Related Events, Time to Progression, and Survival in Patients with Bone-Dominant Metastatic Breast Cancer. *J Nucl Med.* 2018;59:1823-1830.

43. Eisenhauer EA, Therasse P, Bogaerts J, et al. New response evaluation criteria in solid tumours: revised RECIST guideline (version 1.1). *Eur J Cancer.* 2009;45:228-247.

44. Winston CB, Hadar O, Teitcher JB, et al. Metastatic lobular carcinoma of the breast: patterns of spread in the chest, abdomen, and pelvis on CT. *AJR Am J Roentgenol.* 2000;175:795-800.

45. Ulaner GA, Saura C, Piha-Paul SA, et al. Impact of FDG PET Imaging for Expanding Patient Eligibility and Measuring Treatment Response in a Genome-Driven Basket Trial of the Pan-HER Kinase Inhibitor, Neratinib. *Clin Cancer Res.* 2019;3:666-671.

46. Ulaner GA, Goldman DA, Gonen M, et al. Initial Results of a Prospective Clinical Trial of 18F-Fluciclovine PET/CT in Newly Diagnosed Invasive Ductal and Invasive Lobular Breast Cancers. *J Nucl Med.* 2016;57:1350-1356.

47. Tade FI, Cohen MA, Styblo TM, et al. Anti-3-18F-FACBC (18F-Fluciclovine) PET/CT of Breast Cancer: An Exploratory Study. *J Nucl Med.* 2016;57:1357-1363.

48. Ulaner GA, Goldman DA, Corben A, et al. Prospective Clinical Trial of 18F-Fluciclovine PET/CT for Determining the Response to Neoadjuvant Therapy in Invasive Ductal and Invasive Lobular Breast Cancers. *J Nucl Med.* 2017;58:1037-1042.

FIGURES

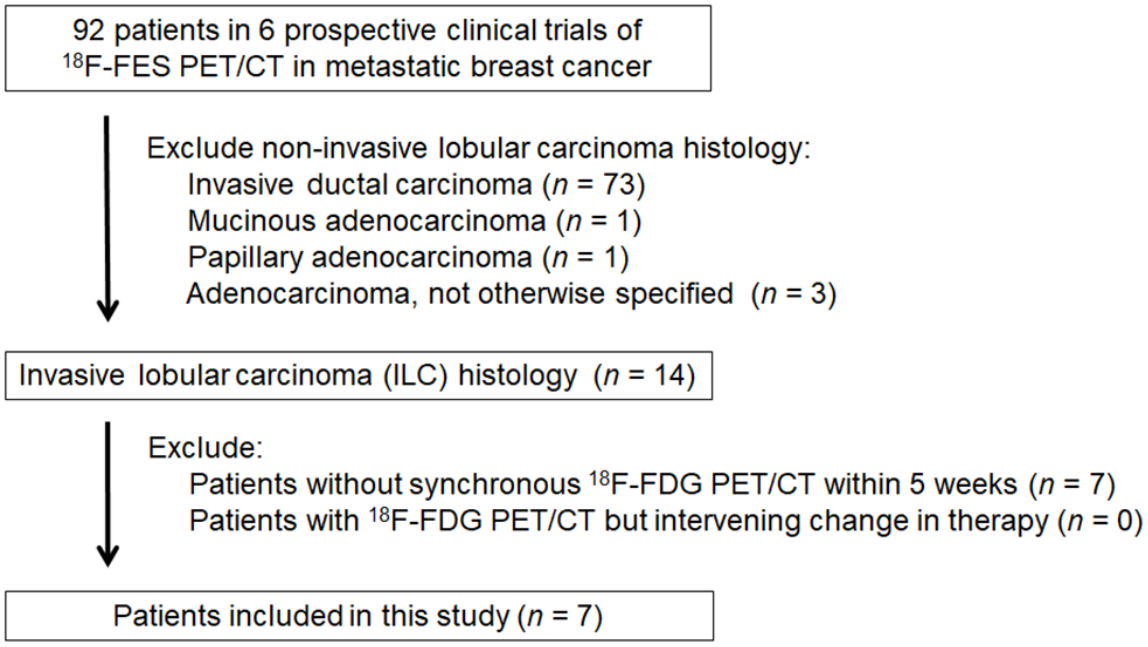

FIGURE 1. Standards for Reporting of Diagnostic Accuracy Studies (STARD) diagram for patients screened in this study.

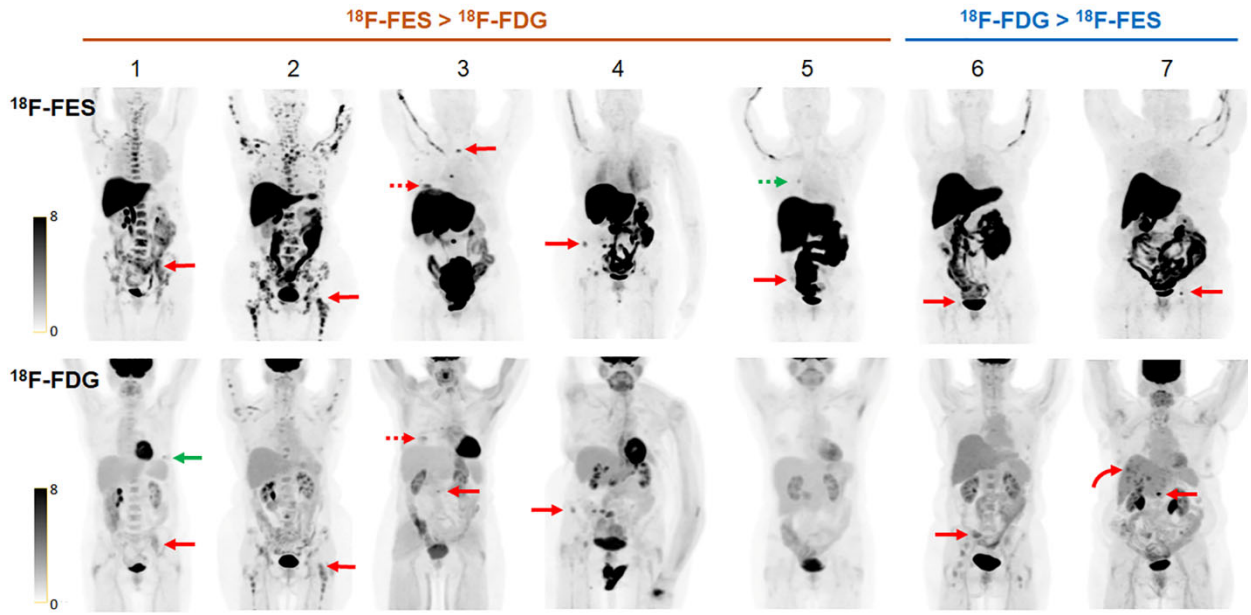

FIGURE 2. Comparison of ^{18}F-FES PET and ^{18}F-FDG PET in seven patients with metastatic ILC. Maximum-intensity projection (MIP) images from ^{18}F-FES PET scans (top row) and ^{18}F-FDG PET scans (bottom row) within five weeks.

In the first five patients, ^{18}F-FES PET detected more metastatic lesions and demonstrated higher SUVs for metastatic lesions than ^{18}F-FDG. In patients 1-5, more osseous metastases (red arrows) are seen on ^{18}F-FES PET than on ^{18}F-FDG PET. In particular, for patient 5, osseous disease is detected on ^{18}F-FES PET but not apparent on ^{18}F-FDG. In patient 3, known recurrence in the breast (dashed red arrows) demonstrates greater SUVmax on ^{18}F-FES than on ^{18}F-FDG. In patient 1, ^{18}F-FDG avidity around a breast implant (green arrow) is probably benign. In patient 5, a right hilar focus is of unclear etiology (dashed green arrow).

In the last two patients, ^{18}F-FDG PET detected more metastatic lesions than ^{18}F-FES PET. In patient 6, more osseous metastases (red arrows) are seen on ^{18}F-FDG PET than ^{18}F-FES PET. In patient 7, more osseous metastases (red arrows) are seen on ^{18}F-FES PET, but multiple liver metastases (curved red arrow) are only seen on ^{18}F-FDG PET.

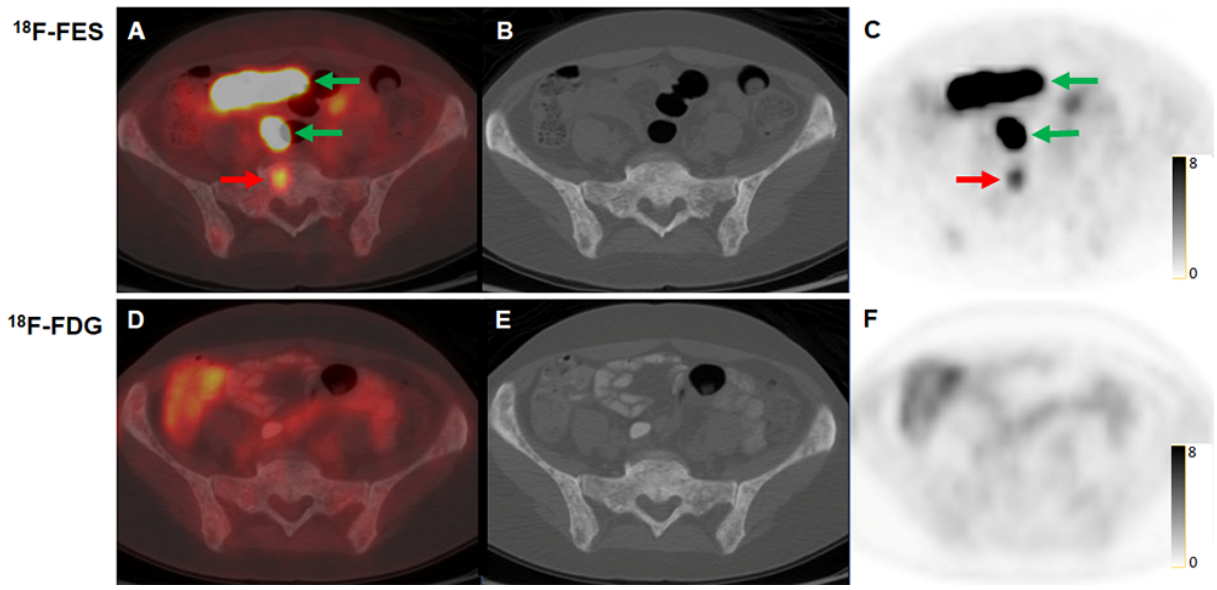

FIGURE 3. Metastatic disease apparent on ^{18}F-FES PET but not on ^{18}F-FDG PET in a 48-year-old woman with biopsy-proven metastatic ILC (patient 5). Axial fused ^{18}F-FES PET/CT (A), CT (B), and ^{18}F-FES PET (C) demonstrates ^{18}F-FES-avid osseous foci (red arrow), consistent with avid malignancy. Physiologic activity was also seen in the bowel (green arrows). Axial fused ^{18}F-FDG PET/CT (D), CT (E), and ^{18}F-FDG PET (F) did not demonstrate any FDG-avid foci suspicious for malignancy.

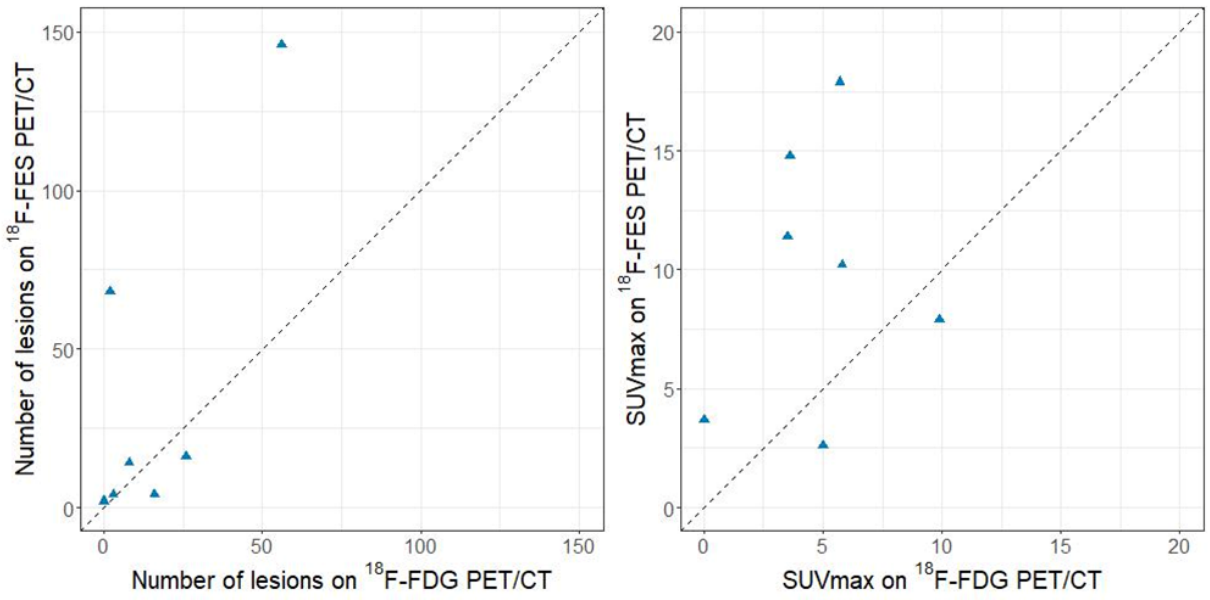

Figure 4. Comparison of lesions on ^{18}F-FES PET/CT and ^{18}F-FDG PET/CT in seven patients with metastatic lobular breast cancer. (A) Comparison of number of avid lesions suspicious for malignancy. (B) Comparison of SUVmax of suspicious lesions. In 5 of 7 patients, more lesions were detected and SUVmax values were higher on ^{18}F-FES PET/CT than on ^{18}F-FDG PET/CT.

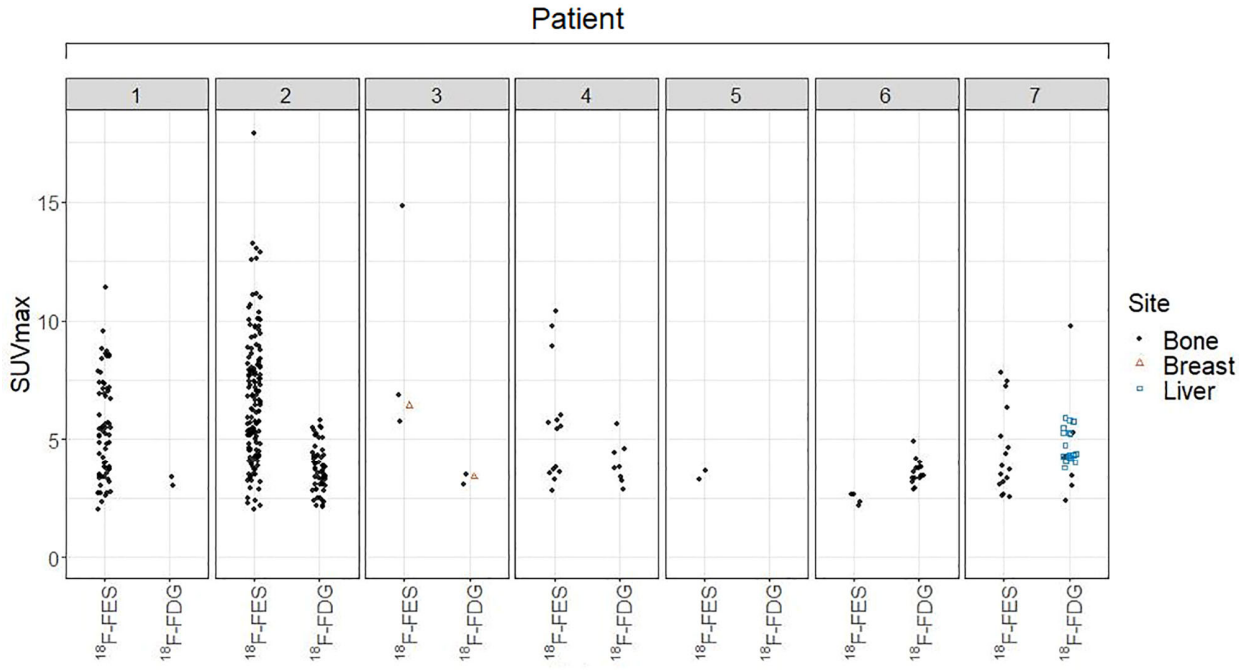

Figure 5. Graphical depiction of SUVmax values for all avid malignancy in all PET/CT scans. There was no FDG avid malignancy in patient 5. The majority of metastases were osseous, represented by black circles. Patient 3 had a breast lesion, represented by orange triangles. Patient 7 had hepatic metastases seen on ^{18}F-FDG, represented by blue boxes.

Table 1. Summary of malignancy seen on ^{18}F-FES and ^{18}F-FDG PET/CT in seven patients with metastatic ER+/PR+/HER2- ILC. * Location of the osseous lesion demonstrating the SUVmax. L = left. R = right. Acet = Acetabulum. Sac = sacrum. VB = vertebral body. N/A = not applicable. The location of the osseous lesion demonstrating the SUVmax is noted by the red arrows in Figure 1. At the bottom of the table are the Liver background (bg) SUVmax and SUVmean values for each scan.

Patient #	**1**		**2**		**3**		**4**		**5**		**6**		**7**	
Age (years)	**67**		**64**		**67**		**66**		**48**		**54**		**69**	
	FES	**FDG**	**FES**	**FDG**	**FES**	**FDG**	**FES**	**FDG**	**FES**	**FDG**	**FES**	**FDG**	**FES**	**FDG**
Days between scans	30		11		13		16		30		35		19	
Bone														
# of foci	68	2	146	56	3	2	14	8	2	0	4	16	16	6
SUVmax	11.4	3.5	17.9	5.7	14.8	3.6	10.2	5.8	3.7	N/A	2.6	5.0	7.9	9.9
Location*	L4 VB	L ilium	R femur	R femur	L3 VB	L3 VB	Sac	Sac	R ilium	N/A	R acet	Sac	L acet	L1 VB
Breast														
# of foci					1	1								
SUVmax					6.5	3.3								
Liver														
# of foci													0	20
SUVmax													N/A	5.9
Liver bg SUVmax	13.8	2.5	15.4	3.1	15.4	2.2	22.9	2.8	12.5	2.2	14.3	3.8	17.0	3.5
Liver bg SUVmean	10.6	2.2	13.8	2.8	13.9	1.9	20.3	2.6	11.7	2.0	12.4	3.5	15.0	3.1